

## Chemical and Stereochemical Actions of UDP–Galactose 4-Epimerase

PERRY A. FREY\* AND ADRIAN D. HEGEMAN†

*Department of Biochemistry, University of Wisconsin—Madison,  
1710 University Avenue, Madison, Wisconsin 53705, United States*

RECEIVED ON SEPTEMBER 5, 2012

### CONSPECTUS

Uridine(5′)diphospho(1)α-D-galactose (UDP-gal) provides all galactosyl units in biologically synthesized carbohydrates. All healthy cells produce UDP-gal from uridine(5′)diphospho(1)α-D-glucose (UDP-glc) by the action of UDP-galactose 4-epimerase (GalE). This Account provides our recent results describing unusual mechanistic features of this enzyme.

Fully active GalE is dimeric and contains one tightly bound nicotinamide adenine dinucleotide (NAD) per subunit. The NAD undergoes reversible reduction to NADH in the chemical mechanism. GalE displays unusual enzymological, chemical, and stereochemical properties. These include practically irreversible binding of NAD, nonstereospecific hydride transfer, uridine nucleotide-induced activation of NAD, Tyr149 as a base catalyst, and [GalE-NADH]-oxidation in one-electron steps by one-electron acceptors.

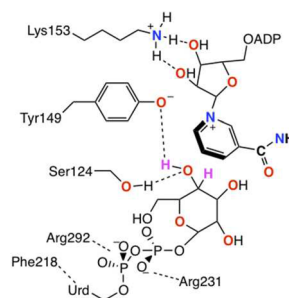
Early studies revealed that uridine(5′)diphospho(1)α-D-4-ketopyranose (UDP-4-ketopyranose) and NADH are reaction intermediates. Weak binding of the 4-ketopyranosyl moiety and strong binding of the UDP-moiety allowed either face of the 4-ketopyranosyl moiety to accept hydride from NADH.

In crystal structures of GalE, NAD bound within a Rossmann-type fold and uridine nucleotides within a substrate domain. Structures of [GalE-NADH] in complex with UDP-glc show Lys153, Tyr149, and Ser124 in contact with NAD or glucosyl-C4(OH). Lys153 forms hydrogen bonds to the ribosyl-OH groups of NAD. The phenolate of Tyr149 is associated with both the nicotinamide ring of NAD and glucosyl-C4(OH). Ser124 is hydrogen-bonded to glucosyl-C4(OH). Spectrophotometry studies show a pH-dependent charge transfer (CT) complex between Tyr149 and NAD. The CT-complex has a  $pK_a$  of 6.1, which results in bleaching of the CT-band. The CT-band also bleaches upon binding of a uridine nucleotide. Kinetic experiments with wild-type GalE and Ser124Ala-GalE show the same kinetic  $pK_a$  values as the corresponding CT-band  $pK_a$ , which point to Tyr149 as the base catalyst for hydride transfer.

We used NMR studies to verify that uridine nucleotide binding polarizes nicotinamide  $\pi$ -electrons. The binding of uridine(5′)-diphosphate (UDP) to GalE-[nicotinamide-1- $^{15}\text{N}$ ]NAD shifts the  $^{15}\text{N}$ -signal upfield 3 ppm, whereas UDP-binding to GalE-[nicotinamide-4- $^{13}\text{C}$ ]NAD shifts the  $^{13}\text{C}$ -signal downfield by 3.4 ppm. Electrochemical and  $^{13}\text{C}$  NMR data for a series of *N*-alkylnicotinamides show that the 3.4 ppm downfield  $^{13}\text{C}$ -perturbation in GalE corresponds to an elevation of the NAD reduction potential by 150 mV. These results account for the uridine nucleotide-dependence in the reduction of [GalE-NAD] by glucose or  $\text{NaBH}_3\text{CN}$ .

Kinetics in the reduction of Tyr149Phe- and Lys153Met-GalE-NAD implicate Tyr149 and Lys153 in the nucleotide-dependent reduction of NAD. They further implicate electrostatic repulsion between N1 of NAD and the  $\epsilon$ -aminium group of Lys153 in nucleotide-induced activation of NAD.

In an  $\text{O}_2$ -dependent reaction, [GalE-NADH] reduces the stable radical UDP-TEMPO with production of superoxide radical. The reaction must proceed by way of a NAD-pyridinyl radical intermediate.



### 1. Introduction

UDP-galactose 4-epimerase (GalE) is essential in galactose metabolism. All healthy cells contain this enzyme. GalE catalyzes eq 1, the conversion of uridine(5′)diphospho(1)-α-D-glucose (UDP-glc) into uridine(5′)diphospho(1)α-D-galactose (UDP-gal). This apparently simple equilibration of

configurations *S* and *R* at C4 of the pyranosyl rings raises mechanistic questions that have stimulated research during 50 years. UDP-gal is the galactosyl donor in complex carbohydrate biosynthesis. GalE is the only enzyme that catalyzes the interconversion of glucosyl and galactosyl groups.

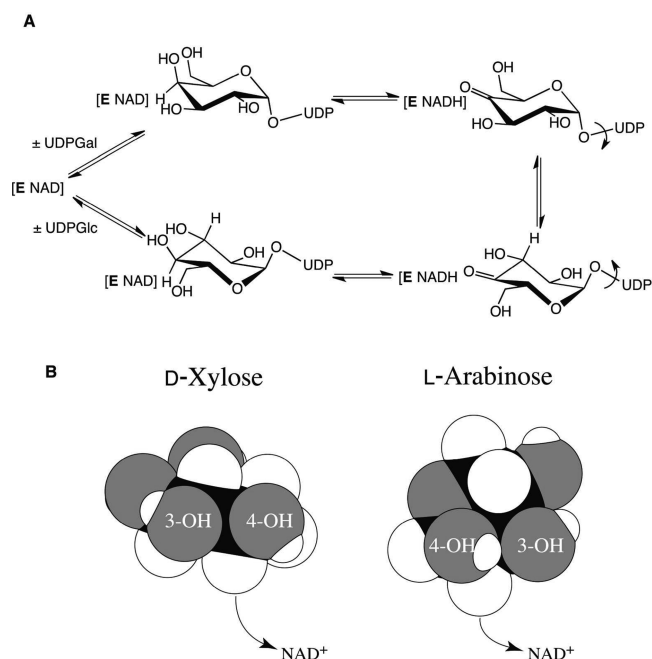
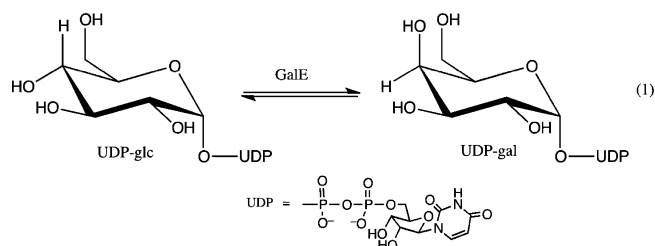


**FIGURE 1.** Nonstereospecific hydride transfer by GalE.



An issue is how nonstereospecificity is brought about by racemases and epimerases. Enzyme–substrate interactions are almost universally stereospecific and lead to stereospecificity in reactions. Figure 1A shows how nonstereospecificity is brought about by GalE, which has one molecule of nicotinamide adenine dinucleotide (NAD) per subunit that functions in reversible redox catalysis. The uridine(5′)diphosphoryl group of the 4-ketopyranosyl intermediate binds very tightly to [GalE-NADH] ( $-7 \text{ kcal mol}^{-1}$ ), whereas the 4-ketopyranosyl moiety binds weakly ( $-2 \text{ kcal mol}^{-1}$ ). This allows torsional mobility for the 4-ketopyranosyl group and nonstereospecific hydride transfer at C4. Figure 1B shows the near congruence of C3(OH), C4(OH), and C4(H) in the rotamers of epimeric substrates uridine(5′)diphospho(1)- $\alpha$ -D-xylose and uridine(5′)diphospho(1)- $\alpha$ -L-arabinose.<sup>1</sup>

## 2. Molecular Structure<sup>‡</sup>

**2.1. Chain Fold and Domains.** Molecular structures of GalE are briefly reviewed by Holden et al.<sup>2</sup> Structures of GalE

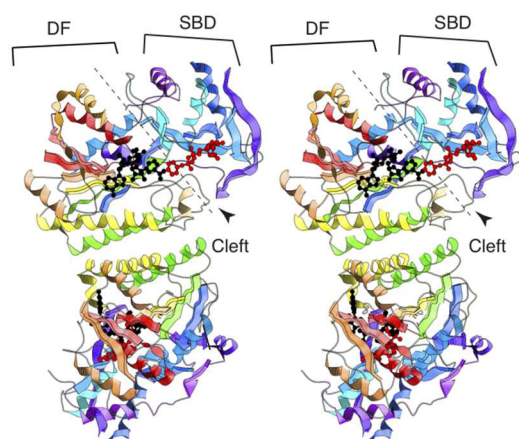


**FIGURE 2.** Ribbon diagram of the GalE chain fold from PDB file 2UDP using MolView.<sup>7</sup>

from *Escherichia coli* in various states of complexation with substrates and inhibitors are available.<sup>3–6</sup> The structure with uridine(5′)diphospho(1)-phenol (UDP-phenol) at the active site (Figure 1) reveals the overall chain fold, and the locations of NADH and UDP-phenol and the relative orientations of the subunits. The subunit interface occurs along two parallel  $\alpha$ -helices, Pro93 to Met111 and Pro148 to Gln167, from each subunit with a rough axis of symmetry in the interface plane and perpendicular to the helices.

Each subunit comprises two domains, a dinucleotide fold (DF) characteristic of NAD-binding enzymes, and a smaller substrate-binding domain (SBD). NAD binds along the C-terminal edge of the twisted  $\beta$ -sheet in the DF and appears as the black ball and stick model in Figure 2. A cleft at the domain interface forms the active site. UDP-phenol, the red ball and stick model, binds to the SBD. Binding of NAD and UDP-phenol project the nicotinamide and phenyl rings into the hydride transfer site. The overall chain fold of human GalE is similar to that of *E. coli* GalE.<sup>8</sup>

**2.2. Binding of NAD.** *E. coli* GalE binds NAD with very high affinity. The purified enzyme contains a full complement of NAD. NAD can be resolved from the enzyme upon denaturation in concentrated guanidinium hydrochloride, and renaturation proceeds upon dilution in the presence of NAD binding to the fully active holoenzyme.<sup>9</sup> GalE shares tight NAD binding with other enzymes that use NAD as a reversible redox coenzyme.<sup>10–15</sup>

The tight [GalE-NADH] binding interactions emerge from the crystal structure.<sup>6</sup> The most striking feature of the [GalE-NADH] contact surface is the extensive hydrogen bonding between the adenosyl moiety and the protein. All but one of the available N and O atoms in the adenosyl moiety are hydrogen bonded to one or two side chain or main chain

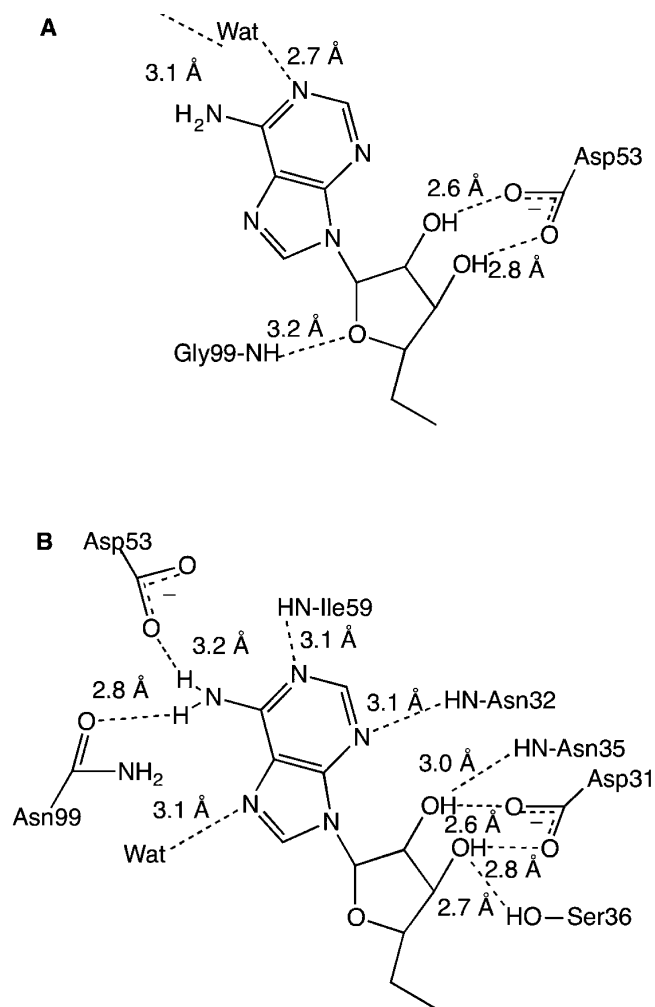


**FIGURE 3.** Contacts between the adenosine in NAD and (A) lactate dehydrogenase or (B) GalE; from PDB files 9LDT and 1XEL using MolView.<sup>7</sup>

enzymatic heteroatoms. Eight such contacts distinguish the [GalE-NADH] structure from those of numerous alcohol dehydrogenase–NAD complexes. The hydrogen bonds between the adenosyl group of NAD in lactate dehydrogenase (LDH) in Figure 3A are compared with those for GalE in Figure 3B. In LDH, only two enzymatic residues form hydrogen bonding contacts to the ribosyl moiety of NAD. Extensive GalE-adenosyl hydrogen bonding and minimal solvation seems to explain the tight binding of NAD to GalE.

Extensive hydrogen bonding to the adenosyl moiety of NAD may be a general feature of enzymes that use NAD as a transiently reduced coenzyme, in which NADH remains bound to the active site throughout the catalytic cycle.<sup>11,15</sup> Retention of NAD in the free enzyme enables these enzymes to display activity without competition from other enzymes that use NAD as a substrate.

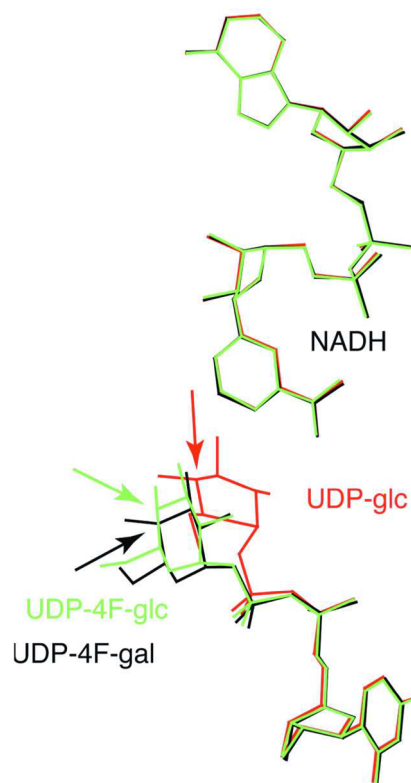


**FIGURE 4.** Structures of uridine(5')diphospho(1)α-D-sugars bound to GalE from PDB files 1XEL, 1UDA, and 1UDB using Molview.<sup>7</sup>

### 3. Structural Support for Glycosyl Mobility

Nonstereospecific hydride transfer in Figure 1 depends on the concept of strong binding of the UDP moiety and weak binding of the sugar moiety of substrates to GalE.<sup>1</sup> Crystallographic analysis of [GalE-NADH-UDP-sugars] further supports this idea. Crystal structures of abortive complexes containing [GalE-NADH] and UDP-glc, uridine(5')diphospho(1)α-D-4-deoxy-4-fluoroglucose (UDP-4F-glc), or uridine(5')diphospho(1)α-D-4-deoxy-4-fluorogalactose (UDP-4F-gal) showed the pyranosyl rings to be oriented differently within the pyranosyl binding site, as shown in Figure 4.<sup>16,17</sup> In contrast, the heavy atoms of the uridine(5')diphosphoryl moieties occupied virtually identical positions in the nucleotide subsite. The structures showed sufficient space in the pyranosyl subsite to allow various orientations of the pyranosyl rings, and differences could be accommodated by torsion about the bond linking the anomeric oxygen and the β-phosphate group of UDP.

### 4. Active Site Structure and Function

**4.1. Lysine 153, Serine 124, and Tyrosine 149.** The side chains of Lys153, Tyr149, and Ser124 in Figure 5 are in hydrogen bonding contact with NADH or UDP-glc in the abortive complex of [GalE-NADH-UDP-glc]. These amino

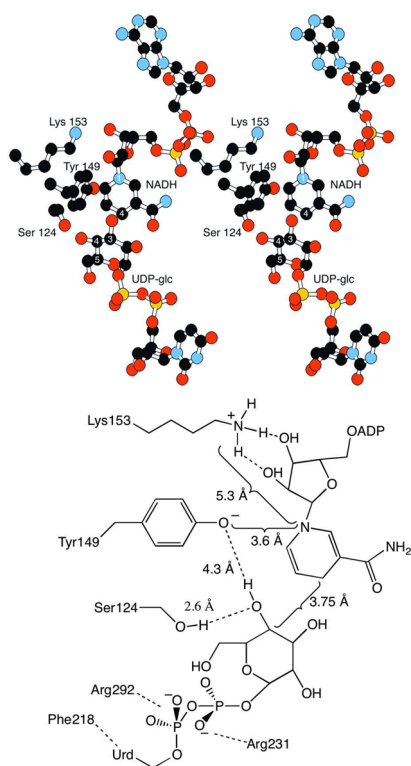


**FIGURE 5.** Active site of [GalE-NADH-UDPGlc]: (top) stereoview; (bottom) 2D schematic.

**TABLE 1.** Kinetic Parameters for GalE in Conversion of UDP-gal to UDP-glc

epimerase	$k_{\text{cat}}$ ( $\text{s}^{-1}$ )	$10^3 K_{\text{m}}$ (M)	$10^{-3} k_{\text{cat}}/K_{\text{m}}$ ( $\text{M}^{-1} \text{s}^{-1}$ )
wild-type	760	0.23	$3.4 \times 10^3$
Lys153Met	0.67	0.083	8.1
Tyr149Phe	0.073	0.026	2.9
Ser124Ala	0.61	0.11	5.5
Ser124Thr	250	0.260	970

acids, Tyr149 and Lys153 in particular, constitute a defining primary sequence element for the short chain dehydrogenase/reductase superfamily<sup>18–20</sup> and are critically important for GalE activity (Table 1). The global structures with Tyr149 changed to phenylalanine (Tyr149Phe-GalE) or Ser124 changed to alanine (Ser124Ala-GalE) are similar to the wild-type GalE, as shown by X-ray crystallography, but the active sites differ by the absence of the hydroxyl groups.<sup>21,22</sup> Inasmuch as NAD is weakly bound upon mutation of Lys153 to methionine (Lys153Met-GalE),<sup>23</sup> the structure seems to be perturbed by the absence of Lys153. The  $\epsilon$ -aminium group of Lys153 contributes significantly to binding NAD through hydrogen bonding with the 2'-OH and 3'-OH groups of the nicotinamide ribosyl ring.

**4.2. Charge Transfer Complexation between NAD and Tyr149.** The UV/vis spectrum of [GalE-NAD] revealed

a spectral feature extending from 300 to 360 nm.<sup>9</sup> This low-intensity absorption did not correspond to the line shape of NADH, and the enzyme did not exhibit the fluorescence characteristic of NADH upon excitation at 340 nm. The band was assigned to a charge transfer complexation, presumably by NAD. The charge transfer band was bleached by addition of uridine(5')-phosphate (UMP) or uridine(5')-diphosphate (UDP), which was taken as evidence of a uridine nucleotide-induced conformational change.

The refined GalE structures revealed the proximity of Tyr149 to the positively charged nicotinamide ring of NAD and the  $\epsilon$ -aminium group of Lys153. The structures also showed Tyr149 in position to serve as a base catalyst for hydride transfer from hexopyranosyl-C4(OH) of substrates. Earlier biochemical efforts to identify the base failed to produce any evidence for the importance of conventional bases in amino acid side chains.<sup>24,25</sup>

Because the phenolic group of free tyrosine ( $\text{pK}_{\text{a}}$  10.1) is not normally basic, consideration of Tyr149 as a possible base forced an assessment of its acid–base properties. In the microenvironment of the active site, the positive electrostatic field created by the proximity of nicotinamide-N1 of NAD and the  $\epsilon$ -aminium group of Lys153 would stabilize the anionic phenolate form of the adjacent Tyr149. Such an interaction would provide a chemical potential for Tyr149 to undergo ionization at physiological pHs, that is, its  $\text{pK}_{\text{a}}$  might be depressed. The potentiality of Tyr149 as a phenolate ion in neutral solution also offered a rationale for p– $\pi$  charge transfer complexation with NAD. Bleaching of the charge transfer band by pH adjustment below 6 or by mutation of Tyr149 to Phe149 supported the assignment of charge transfer complexation by Tyr149.<sup>21</sup>

The pH dependence of the charge transfer intensity for wild-type (wt) GalE corresponds to a  $\text{pK}_{\text{a}}$  of 6.1 for Tyr149. The results for variants mutated at Ser124 to threonine, alanine, or valine are as follows: Ser124Thr,  $\text{pK}_{\text{a}}$  6.3; Ser124Ala,  $\text{pK}_{\text{a}}$  6.7; Ser124Val,  $\text{pK}_{\text{a}}$  6.9.<sup>21</sup> The effects of mutating Ser124 on the  $\text{pK}_{\text{a}}$  of Tyr149 cannot be interpreted without structural information because mutation of a single amino acid can in principle trigger global conformational changes. The X-ray crystallographic analyses of the Thr124, Ala124, and Val124 variants reveal no significant conformational differences from the wild-type Ser124-GalE. Therefore, variations in  $\text{pK}_{\text{a}}$  of Tyr149 in wild-type and variants should be attributed to microenvironmental differences among the amino acid side chains at position 124.

The barrier to ionization of neutral acids such as phenols increases with decreasing polarity of the medium because of

increasing energy barrier for charge separation upon release of a proton. The side-chain structures of the variant amino acids are as follows: serine,  $-\text{CH}_2\text{OH}$ ; threonine,  $-\text{CH}(\text{OH})\text{CH}_3$ ; alanine,  $-\text{CH}_3$ ; and valine,  $-\text{CH}(\text{CH}_3)_2$ . The order of decreasing polarity in the series is  $-\text{CH}_2\text{OH} > -\text{CH}(\text{OH})\text{CH}_3 > -\text{CH}_3 > -\text{CH}(\text{CH}_3)_2$ . This order represents decreasing active site polarity in the variant series Ser124(wt) > Ser124Thr > Ser124Ala > Ser124Val. The order of decreasing polarity accounts for the order of increasing  $\text{pK}_a$  for Tyr149 as listed above.<sup>21</sup> The  $\text{pK}_a$ 's are thermodynamic values for Tyr149 in the free enzymes.

**4.3. Acid–Base Catalysis of Hydride Transfer.** Tyr149 and Ser124 appear to be in position to participate in the acid–base catalysis required to drive hydride transfer. One or both presumably facilitate the abstraction of a proton from pyranosyl-C4(OH) in concert with transfer of C4-hydride to NAD. Both Tyr149 and Ser124 are important for activity (Table 1), with Tyr 149 being more important. The only available structures with bound nucleotide sugars are those of abortive complexes [GalE-NADH-UDP-glc]. Abortive complexes are inactive because of noncomplementary species of pyridine nucleotide (NADH) and UDP-sugars, so these structures cannot be used to define exactly how base catalysis takes place. The structural relationships among the glucosyl ring, Tyr149, and Ser124 might be different in the Michaelis complex with UDP-glc, [GalE-NAD-UDP-glc].

The contributions of Tyr149 and Ser124 to hydride transfer are synergistic, suggesting that they act in concert. This conclusion arises from kinetic studies of mutated GalEs. The maximum activity of doubly mutated Tyr149Phe/Ser124Ala-GalE is about  $10^{-7}$  times that of the wild type GalE.<sup>26</sup> This low activity corresponds to the product of the lowering in activity brought about by mutating Tyr149 to Phe ( $10^{-4}$ ) and Ser124 to Ala ( $3 \times 10^{-3}$ ). Structural analysis showed these mutations to have little effect on the overall conformations of the variants, which differed essentially by the absence of the side chain hydroxyl groups. Thus, double mutation is kinetically multiplicative rather than additive, whereas the activation energy barriers are additive.

Steady-state pH-rate analysis of wild-type and variant GalEs confirm that Tyr149 functions as the base catalyst for hydride transfer.<sup>26</sup> Epimerization by wild-type GalE is pH independent for both  $k_{\text{cat}}$  and  $k_{\text{cat}}/K_m$  between pH 5.5 and 9.5. Hydride transfer is not rate limiting in this pH range, as shown by the absence of a kinetic-isotope effect in the reaction of UDP-gal-*d*<sub>7</sub>. Epimerization by Tyr149Phe-GalE is also pH independent for  $k_{\text{cat}}$ , but the plot of  $\log(k_{\text{cat}}/K_m)$  turns down at lower pHs with a kinetic  $\text{pK}_a$  of 7.1. No kinetic

isotope effect is observed in the reaction of UDP-gal-*d*<sub>7</sub> at pH 8.3, above the kinetic  $\text{pK}_a$ ; however, the deuterium kinetic isotope effect at pH 6.2 is 2.2. The simplest interpretation is that activity is affected by an ionizing group with a  $\text{pK}_a$  higher than 7.1 in the free enzyme. The observed kinetic  $\text{pK}_a$  of 7.1 arises from the fact that hydride transfer is not rate limiting at higher pHs.<sup>27,28</sup> We shall discuss the probable identity of this group below.

The pH–rate profile for epimerization by the variant Ser124Ala-GalE is particularly informative. Both  $k_{\text{cat}}$  and  $k_{\text{cat}}/K_m$  display pH dependencies between pH 6 and 9, and epimerization of UDP-gal-*d*<sub>7</sub> proceeds with a deuterium kinetic isotope effect of 2.1 throughout this pH range, suggesting that hydride transfer is the major contributing step to rate limitation throughout the pH range. The pH-dependencies correspond to kinetic  $\text{pK}_a$ 's of 6.3 for  $k_{\text{cat}}$  and 6.7 for  $k_{\text{cat}}/K_m$ . The value of 6.7 for  $k_{\text{cat}}/K_m$  is particularly significant because it refers to free Ser124Ala-GalE and is the same value as the thermodynamic  $\text{pK}_a$  of Tyr149 in this variant. It is reasonable to assign this  $\text{pK}_a$  to Tyr149 in free Ser124Ala-GalE and the value of 6.3 to Tyr149 in the Michaelis complex. These pH dependencies strongly support the assignment of Tyr149 to base catalysis of hydride transfer in the Ser124Ala-GalE variant.

Additional evidence with wild-type GalE bolsters the assignment of Tyr149 as the base catalyst for hydride abstraction. Uridine(5')diphospho(6)glucose, a regio-isomer of UDP-glc in which glucose is bonded to UDP through C6(O), irreversibly reduces [GalE-NAD] with rate-limiting hydride transfer from C1(H).<sup>29</sup> Investigation of the pH dependence of this reduction produced a bell-shaped pH–rate profile with breaks at  $\text{pK}_a$ 's of 6.1 and 9.2. The  $\text{pK}_a$  of 6.1 could be attributed to base catalysis of hydride transfer, but it could not be assigned to an amino acid side chain until structural information became available. Knowledge of the presence of Tyr149 in the active site, the kinetic  $\text{pK}_a$  of 6.1 for hydride transfer to UDP-6-glucose, and the thermodynamic  $\text{pK}_a$  of 6.1 for Tyr149 allows the assignment of Tyr149 as the base catalyst in wild-type GalE.

The structures of *E. coli* abortive complexes are consistent with several hydrogen-bonding networks in the Michaelis complexes. The two mechanisms of base-catalyzed hydride transfer in Figure 6 attribute the main driving force for base catalysis to Tyr149, but they differ in the role of Ser124. Tyr149 can function as a base in this case because it displays a  $\text{pK}_a$  value of 6.1 and it is ionized in neutral solution.<sup>21</sup> In mechanism A, the phenolate group of Tyr149 abstracts the proton from C4(OH) of the glucosyl moiety, and the C4(OH)

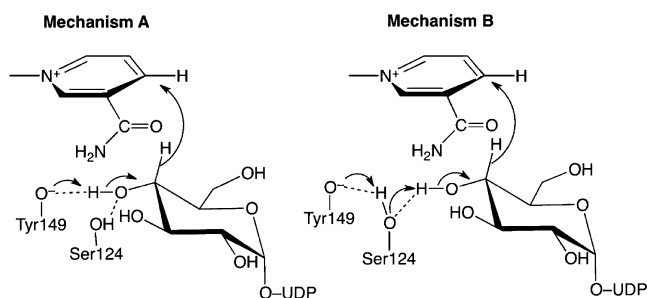


**FIGURE 6.** Mechanisms for participation of Ser124 and Tyr149 in GalE-hydride transfer.

group is hydrogen bonded to Tyr149 and Ser124. In mechanism B, the hydroxyl group of Ser124 intervenes between Tyr149 and the glucosyl-C4(OH) group, and Ser124 mediates proton transfer by a relay mechanism. The structure of the *E. coli* abortive complex seems to be more consistent with mechanism B, whereas the structure of the human abortive complex is more consistent with mechanism A.<sup>8</sup> Both mechanisms A and B in Figure 6 are compatible with the concerted functions of Tyr149 and Ser124.

Now consider the kinetic  $pK_a$  of 7.1 for  $k_{cat}/K_m$  in epimerization by Tyr149Phe-GalE. The absence of a deuterium kinetic isotope effect above the  $pK_a$  coupled with the observation of an isotope effect below the  $pK_a$  proves that the kinetic  $pK_a$  arises from a change in rate-determining step between pH 6.2 and 8.3. However, hydride transfer requires base catalysis, so a basic entity must participate in the mechanism. In cases of pH-dependent kinetic isotope effects such as this, the thermodynamic  $pK_a$  of such a base must be higher than the kinetically measured  $pK_a$  of 7.1.<sup>27,28</sup>

With phenylalanine in place of tyrosine at position 149 in Tyr149Phe-GalE, catalysis by tyrosine is not possible, but Ser124 remains in position and has access to the C4(OH) of the substrate hexopyranosyl group. Base catalysis by Ser124 in that case is less unlikely than it might seem. There is reason to expect the  $\beta$ -OH group of Ser124 in Tyr149Phe-GalE to ionize with a much lower  $pK_a$  than the value of 13.4 typical of serine. The positive electrostatic field created by the  $\epsilon$ -aminium group of Lys153 and nicotinamide-N1 of NAD remains in place, and the hydrophobicity of the site is greater than in the wild-type enzyme owing to the absence of the phenolate group of Tyr149. In wild-type GalE, the positive electrostatic field lowers the  $pK_a$  of Tyr149 by about 4 units. In Tyr149Phe-GalE, it should lower the  $pK_a$  of Ser124 comparably or more to  $\leq 9.4$ , a value that is higher than the kinetic value of 7.1, as required by theory, but still low enough to be potentially effective in catalysis.

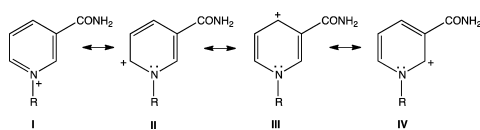
The variant Lys153Met-GalE also displays very low activity, about 1/1000th that of wild-type enzyme in terms of  $k_{cat}$  and a modest decrease in  $K_m$  (Table 1). As will be discussed in the following section, the electrostatic interaction of Lys153 with the positive charge on the nicotinamide ring is thought to be important in enhancing the reactivity of NAD.<sup>30</sup>

## 5. Uridine Nucleotide-Induced Activation of NAD

**5.1. Kinetic Evidence of Induced NAD Activation.** UMP-dependent reductive inactivation of GalE by sugars<sup>1</sup> or sodium cyanoborohydride<sup>31</sup> provides clues to the mechanism by which substrates regulate [GalE-NAD] through an induced conformational transition. Such a change could entail the ordering of catalytic groups required to facilitate hydride transfer. Alternatively, it could consist of an alteration in the interactions between the GalE active site and NAD that enhances the reduction potential of NAD. Two lines of evidence support the latter hypothesis. First, the reduction of [GalE-NAD] by  $\text{NaBH}_3\text{CN}$  suggests that UMP binding increases the reactivity of NAD. Hydride transfer by  $\text{NaBH}_3\text{CN}$  is not facilitated by base catalysis, so an ordering of catalytic groups by UMP-binding does not explain increased reactivity of this reducing agent. Moreover,  $\text{NaBH}_3\text{CN}$  is more reactive with the complex [GalE-NAD-UMP] than with free NAD. Higher reactivity relative to NAD in solution toward a nonspecific hydride-reducing agent requires an alteration of the reduction potential of NAD in the active site.

**5.2. Spectroscopic Signals of Induced NAD Activation.** The first spectroscopic evidence of a uridine nucleotide-induced conformational change came in <sup>31</sup>P NMR experiments, which revealed <sup>31</sup>P NMR changes in NAD upon binding UMP.<sup>32</sup> The <sup>31</sup>P-chemical shifts changed from  $-9.6$  and  $-12.2$  ppm in free [GalE-NAD] to  $-10.5$  and  $-11.1$  ppm in the complex [GalE-NAD-UMP].

NMR spectroscopic probing of the nicotinamide ring in [GalE-NAD] revealed a uridine nucleotide-induced electronic polarization of the  $\pi$ -electrons. The binding of UDP to [GalE-[1-<sup>15</sup>N]NAD] caused an upfield displacement of the <sup>15</sup>N NMR signal by 3 ppm, corresponding to increased electronic shielding of N1.<sup>33–35</sup> Furthermore, UDP induced a downfield displacement of the <sup>13</sup>C NMR signal by 3.4 ppm upon binding to [GalE-[4-<sup>13</sup>C]NAD]. The <sup>15</sup>N chemical shift was unaffected by UDP when the label was in the carboxamide group of NAD. The UDP-induced downfield displacements of the <sup>13</sup>C NMR signals for GalE-[2-<sup>13</sup>C]NAD and GalE-[6-<sup>13</sup>C]NAD were found to be 1.4 ppm and 1.3 ppm, respectively.<sup>33</sup>

SCHEME 1<sup>a</sup>

<sup>a</sup>R = adenosine(5')diphospho(1)ribose(5).

The effects of UDP-binding on the NMR spectroscopy and reactivity of [GalE-NAD] can be rationalized in terms of perturbations in electron density within the nicotinamide ring. As illustrated in Scheme 1, the structure can be described as a hybrid of resonance forms.

The forms in Scheme 1 are relevant to this discussion; the carboxamide is excluded because of the absence of any UDP-effect with <sup>15</sup>N-carboxamide. Form **I** dominates the structure; however, the other forms contribute significantly to the hybrid. The results with [1-<sup>15</sup>N]NAD and [4-<sup>13</sup>C]NAD indicate that UDP-binding enhances the importance of form **III** to the hybrid structure.

Contributions of forms **II** and **IV** are smaller. All the data suggest decreased electron density at nicotinamide-carbon centers, especially C4, and increased electron density at N1 upon binding UDP to [GalE-NAD]. The results indicate that increased reactivity at C4 of NAD toward all hydride reducing agents can be attributed to decreased electron density at C4 upon binding UDP.

In the picture emerging from the <sup>13</sup>C and <sup>15</sup>N NMR data, UDP-binding induces a polarization of electron density away from C4 and toward N1 in the nicotinamide ring.<sup>34</sup> Polarization of this nature would increase the reduction potential of NAD, as well as the reactivity of NAD toward hydride reducing agents.

The foregoing interpretation is further strengthened, albeit indirectly, by structure–reactivity studies of the nicotinamide ring in a series of *N*-alkylnicotinamides. The kinetic reactivities with NaBH<sub>3</sub>CN, the 4-<sup>13</sup>C-chemical shifts, and the reduction potentials of *N*-alkylnicotinamides (N– = CH<sub>3</sub>–, Ph–, *p*-NCPH–, CH<sub>3</sub>O<sub>2</sub>C–, and NC–) are all linearly correlated. The chemical results show that a 3.4 ppm downfield displacement of the 4-<sup>13</sup>C-chemical shift corresponds to a 3000- to 15000-fold increase in reactivity with NaBH<sub>3</sub>CN and a positive shift of 150 mV in reduction potential.<sup>33,35</sup> UMP increases the reactivity of [GalE-NAD] 3000-fold toward reduction by glucose,<sup>36</sup> well within the range indicated by the <sup>13</sup>C NMR results in the structure–reactivity studies. Therefore, uridine nucleotide-dependent reductive inactivation of [GalE-NAD] is brought about by a conformational

TABLE 2. Second-Order Rate Constants for Reductive Inactivation of Epimerase

Epimerase	10 <sup>3</sup> k (M <sup>-1</sup> s <sup>-1</sup> ) {Glc}		10 <sup>3</sup> k (M <sup>-1</sup> s <sup>-1</sup> ) {NaBH <sub>3</sub> CN}	
	+UMP	–UMP	+UMP	–UMP
wild type	78	42	2800	42
Lys153Met	<sup>a</sup>		140	140
Tyr149Phe	0.012		35000	550
Ser124Ala	2.2		2700	18
Ser124Thr	23		2800	5

<sup>a</sup>No reaction.

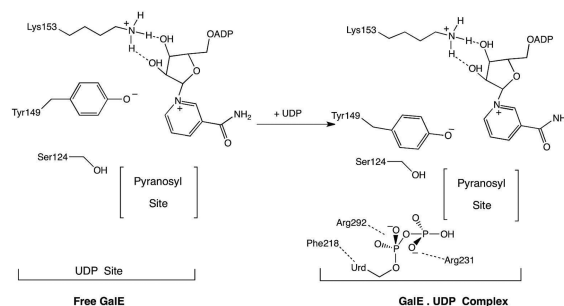


FIGURE 7. A model for UDP-induced activation of NAD in GalE.

change that increases the reduction potential and reactivity of NAD.

**5.3. Roles of Lys153 and Tyr149 in NAD Activation.** Evidence indicates that Lys153 and Tyr149 play key roles in uridine nucleotide dependent reductive inactivation. The first hint appeared in the relative reactivities of NAD in mutated forms of [GalE-NAD] with NaBH<sub>3</sub>CN. Table 2 shows data on UMP-dependent reductive inactivation of GalE mutated at Lys153, Ser124, or Tyr149. The kinetic consequences of mutations on reduction by glucose are analogous to their effects on catalytic activity that appear in Table 1. The results with NaBH<sub>3</sub>CN are markedly different. Reactions of borohydride are not subject to base catalysis, which simplifies the interpretation of results. The reactivity of Lys153Met-GalE with NaBH<sub>3</sub>CN is significantly less than that of wild-type GalE and is not UMP-dependent, proving that Lys153 is involved in activation by UMP.<sup>30</sup> Lys153Ala-GalE displays similar reactivities. NAD in Tyr149Phe-GalE is reduced 12-times faster than in GalE, and UMP enhances the rate by only 60-fold, compared with 800-fold for GalE. Mutation of Ser124 has little effect on the reactivity with NaBH<sub>3</sub>CN. Abolition of either the positive charge of ε-ammonium ion of Lys153 or the negative charge of the Tyr149 phenolate group strikingly affects the reactivity of [GalE-NAD] with NaBH<sub>3</sub>CN and its UMP-dependence.

Any model that explains UMP dependence in reduction of the complex [GalE-NAD-UMP] must be compatible with

the fact that NAD reactivity is enhanced by abolishing the phenolate group of Tyr149 and decreased by abolishing the  $\epsilon$ -aminium group of Lys153. The simplest model is that in Figure 7, where it is postulated that the phenolate group of Tyr149 interacts closely with the nicotinamide ring of NAD in free GalE. The charge transfer band supports this interaction. Lys153 binds the 2'-OH and 3'-OH of the nicotinamide ribosyl moiety of NAD, with the  $\epsilon$ -aminium group placed 5.3 Å from the positively charged quaternary N1 of NAD. Tyr149 partially shields the electrostatic repulsion between nicotinamide-N1 and Lys153 in the resting enzyme. Uridine nucleotide-binding shifts the phenolate of Tyr149 into position to function in base catalysis with the substrate, attenuating the charge transfer interaction.<sup>9</sup> It also decreases the screening by Tyr149 of electrostatic repulsion between the nicotinamide-N1 and Lys153. The enhanced electrostatic repulsion polarizes the  $\pi$ -electron cloud toward nicotinamide-N1 and increases the hydride reactivity at nicotinamide-C4.

Other models might postulate that the interactions of both Lys153 and Tyr149 with NAD change with UDP binding. While the model in Figure 7 is simpler and preferred, it raises questions about the role of Tyr149. Spectroscopic and kinetic experiments implicate Tyr149 in the uridine nucleotide-induced conformational transition. If the model in Figure 7 is correct, the <sup>13</sup>C NMR experiment with [Tyr149Phe-GalE-[4-<sup>13</sup>C]NAD] should give different results than those obtained with GalE. Specifically, there should be no effect of UDP on the chemical shift of nicotinamide-4-<sup>13</sup>C. Moreover, the free mutated enzyme should display the downfield 4-<sup>13</sup>C-signal that is seen with the wild-type GalE only in the presence of UDP. These conditions are confirmed experimentally, with both Tyr149Phe-GalE and the doubly mutated Tyr149Phe/Ser124Ala-GalE.<sup>34</sup> The same experiments with Ser124Ala-GalE gave essentially the same results as the wild-type GalE. All available evidence is consistent with the activation model in Figure 7.

UDP-*N*-acetylgalactosamine 4-epimerases appear to function by a mechanism similar to that of GalE.<sup>37–42</sup>

**5.4. One-Electron Transfer by GalE-NADH.** In a chemically interesting aspect of GalE catalysis, [GalE-NADH] can undergo oxidation in one-electron steps. This is observed when the reduced complex is presented with a substrate that is a one-electron acceptor, uridine(5')diphospho(4)-tetramethylpiperidine-1-yl (UDP-TEMPO), a stable free radical, as illustrated in Figure 8.<sup>43</sup> The reduction of UDP-TEMPO proceeds at the active site of [GalE-NADH] concomitant with the oxidation of NADH in the presence of air and with the

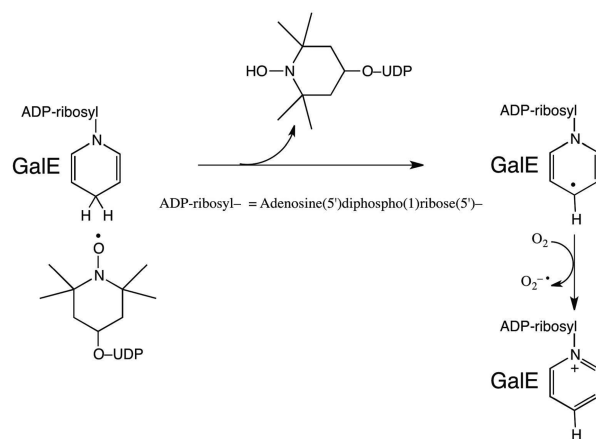


**FIGURE 8.** A mechanism for oxidation of GalE-NADH by dioxygen and UDP-TEMPO.

production of superoxide. No reaction can be observed under anaerobic conditions. A likely mechanism shown in Figure 8 begins with hydrogen transfer from NADH to UDP-TEMPO to produce the pyridinyl radical of NAD, followed by reaction with O<sub>2</sub> to generate NAD and O<sub>2</sub><sup>•-</sup>. One could consider a mechanism in which dioxygen first reacts with [GalE-NADH] to form HO<sub>2</sub><sup>\*</sup> and the pyridinyl radical, which then reduces UDP-TEMPO by electron and proton transfer. The mechanism in Figure 8 is currently preferred because the binding of uridine nucleotides protects [GalE-NADH] from oxidation by dioxygen.

The pyridinyl radical of NAD is stabilized by delocalization of the unpaired electron over nicotinamide-C3, -C4, and -C5 and carboxamido-O and -N. Pyridinyl radicals have been known as stable species for more than 45 years and at one time were considered as possible intermediates in reactions of NAD-dependent oxidoreductases.<sup>44,45</sup> However, physical organic mechanistic analysis of flavin-reduction by *N*-alkyl-1,4-dihydropyridinones strongly implicated hydride transfer as the dominant mechanism.<sup>46,47</sup> This was regarded as a stringent test for one-electron transfer by NADH, owing to the propensity for flavins to undergo electron transfer either in one-electron steps via flavin semiquinone intermediates, or in two-electron mechanisms such as hydride transfer. Most biological reactions of NAD/NADH proceed by hydride transfer, especially alcohol and amine dehydrogenation, in which the alcohol or amine radical intermediates would be very high energy species.

How then to explain the reaction of [GalE-NADH] with UDP-TEMPO? This presents a special case in that both dioxygen and UDP-TEMPO are paramagnetic and obligate one-electron acceptors. The only obvious alternative to mechanisms such as that in Figure 8 would be to postulate



hydride reduction of a protein disulfide bridge by [GalE-NADH], which might then be oxidized by dioxygen and UDP-TEMPO in one-electron steps. However, the structure of GalE does not include a disulfide bridge in either the NAD or the uridine nucleotide binding sites. Therefore, a pyridinyl-radical mechanism appears most likely.

Dehydrogenations by GalE in the 4-epimerase mechanism likely proceed by hydride transfer. However, the reactivity of [GalE-NADH] with dioxygen in the absence of a uridine nucleotide and the reaction of [GalE-NADH] with UDP-TEMPO and dioxygen implicate one-electron mechanisms of [GalE-NADH] oxidation in reactions with paramagnetic species.

#### BIOGRAPHICAL INFORMATION

**Perry Allen Frey** is Professor of Biochemistry Emeritus at the University of Wisconsin—Madison. He trained in Chemistry at The Ohio State University, B.S. 1959, in Biochemistry at Brandeis University, Ph.D. 1968, and as a Postdoctoral Fellow in Chemistry at Harvard University in 1968. He was on the faculty of Chemistry at Ohio State from 1969 to 1981 and moved to the University of Wisconsin—Madison in 1981, where he served as the Robert H. Abeles Professor of Biochemistry until 2008.

**Adrian Daniel Hegeman** is Assistant Professor of Horticultural Science and Plant Biology at the University of Minnesota. He received his undergraduate education at Oberlin College and his Ph.D. degree in Biochemistry at the University of Wisconsin—Madison. He was a postdoctoral fellow in the Biotechnology Center at the University of Wisconsin—Madison before moving to the University of Minnesota.

#### FOOTNOTES

<sup>†</sup>The crystal structures of GalE discussed in this Account were solved in the laboratories of Hazel M. Holden and Ivan Rayment at the University of Wisconsin—Madison.

\*To whom correspondence should be addressed. Telephone: (608) 262-0055. Fax: (608) 265-2904. E-mail: frey@biochem.wisc.edu.

The authors declare no competing financial interest.

<sup>†</sup>Current address: Horticultural Science, University of Minnesota, 1970 Folwell Avenue, Saint Paul, MN 55108-6007.

#### REFERENCES

- Frey, P. A. Complex pyridine nucleotide-dependent transformations. In *Pyridine Nucleotide Coenzymes: Chemical, Biochemical, and Medical Aspects*; Dolphin, D., Poulson, R., Avramovic, O., Eds.; John Wiley & Sons: New York, 1987; Vol 2B, pp 461–511 and references therein.
- Holden, H. M.; Rayment, I.; Thoden, J. B. Structure and function of enzymes of the Leloir pathway for galactose metabolism. *J. Biol. Chem.* **2003**, *278*, 43885–43888.
- Bauer, A. J.; Rayment, I.; Frey, P. A.; Holden, H. M. The molecular structure of UDP-galactose 4-epimerase from *Escherichia coli* determined at 2.5 Å resolution. *Proteins* **1992**, *12*, 372–381.
- Thoden, J. B.; Frey, P. A.; Holden, H. M. High-resolution, H. M. X-ray structure of UDP-galactose 4-epimerase complexed with UDP-phenol. *Protein Sci.* **1996**, *5*, 2149–2161.
- Thoden, J. B.; Frey, P. A.; Holden, H. M. Molecular structure of the NADH/UDP-glucose abortive complex of UDP-galactose 4-epimerase from *Escherichia coli*: Implications for the catalytic mechanism. *Biochemistry* **1996**, *35*, 5137–5144.
- Thoden, J. B.; Frey, P. A.; Holden, H. M. Crystal structures of the oxidized and reduced forms of UDP-galactose 4-epimerase isolated from *Escherichia coli*. *Biochemistry* **1996**, *35*, 2557–2566.
- Smith, T. J. MolView: A program for analyzing and displaying atomic structures on the Macintosh personal computer. *J. Mol. Graphics* **1995**, *13*, 122–125.
- Thoden, J. B.; Wohlers, T. M.; Fridovich-Keil, J. L.; Holden, H. M. Crystallographic evidence for Tyr157 functioning as the active site base in human UDP-galactose 4-epimerase. *Biochemistry* **2000**, *39*, 5691–5701.
- Liu, Y.; Vanhooke, J. L.; Frey, P. A. UDP-galactose 4-epimerase: NAD<sup>+</sup> content and a charge-transfer band associated with the substrate-induced conformational transition. *Biochemistry* **1996**, *35*, 7615–7620.
- Glaser, L.; Zarkowsky, H. Dehydration in nucleotide-linked deoxysugar synthesis. In *The Enzymes*, 3rd ed.; Boyer, P. D., Ed.; Academic Press: New York, 1971; Vol. 5, pp 465–479.
- Mulchack, A. M.; Theisen, M. J.; Essigman, B.; Benning, C.; Garavito, R. M. Crystal structure of SQD1, an enzyme involved in the biosynthesis of the plant sulfolipid headgroup donor UDP-sulfoquinovose. *Proc. Natl. Acad. Sci. U.S.A.* **1999**, *96*, 13097–13102.
- Deacon, A. M.; Ni, Y. S.; Coleman, W. G., Jr.; Ealick, S. E. The crystal structure of ADP-L-glycero-D-mannoheptose 6-epimerase: Catalysis with a twist. *Structure* **2000**, *8*, 453–462.
- Hallis, T. M.; Zhao, Z.; Liu, H.-w. New insights into the mechanism of CDP-D-tylucose 2-epimerase: An enzyme catalyzing epimerization at an unactivated stereocenter. *J. Am. Chem. Soc.* **2000**, *122*, 10493–10503.
- Wolff, E. C.; Wolff, J.; Park, M. H. Deoxyhypusine synthase generates and uses bound NADH in a transient hydride transfer mechanism. *J. Biol. Chem.* **2000**, *275*, 9170–9177.
- Liao, D.-I.; Wolff, E. C.; Park, M. H.; Davies, D. R. Crystal structure of the NAD complex of human deoxyhypusine synthase: An enzyme with a ball-and-chain mechanism for blocking the active site. *Structure* **1998**, *6*, 23–32.
- Thoden, J. B.; Hegeman, A. D.; Wesenberg, G.; Chapeau, M. C.; Frey, P. A.; Holden, H. M. Structural analysis of UDP-sugar binding to UDP-galactose 4-epimerase from *Escherichia coli*. *Biochemistry* **1997**, *36*, 6294–6304.
- Thoden, J. B.; Holden, H. M. Dramatic differences in binding of UDP-galactose and UDP-glucose to UDP-galactose 4-epimerase from *Escherichia coli*. *Biochemistry* **1998**, *37*, 11469–11477.
- Persson, B.; Krook, M.; Jörmvall, H. Short-chain dehydrogenases/reductases. In *Enzymology and Molecular Biology of Carbonyl Metabolism 5*; Weiner, H.; Holmes, R. S.; Wermuth, B., Eds.; Plenum Press: New York, 1995; pp 383–395.
- Baker, M. E.; Blasco, R. Expansion of the mammalian 3-β-hydroxysteroid dehydrogenase/planar dihydroflavonol reductase superfamily to include a bacterial cholesterol dehydrogenase, a bacterial UDP-galactose-4-epimerase, and open reading frames in vaccinia virus and fish lymphocystis disease virus. *FEBS Lett.* **1992**, *301*, 89–93.
- Holm, L.; Sander, C.; Murzin, A. Three sisters, different names. *Nat. Struct. Biol.* **1994**, *1*, 146–147.
- Liu, Y.; Thoden, J. B.; Kim, J.; Berger, E.; Gulick, A. M.; Ruzicka, F. J.; Holden, H. M.; Frey, P. A. Mechanistic roles of tyrosine 149 and serine 124 in UDP-galactose 4-epimerase from *Escherichia coli*. *Biochemistry* **1997**, *36*, 10675–10684.
- Thoden, J. B.; Gulick, A. M.; Holden, H. M. Molecular structures of the S124A, S124T, and S124V site-directed mutants of UDP-galactose 4-epimerase from *Escherichia coli*. *Biochemistry* **1997**, *36*, 10685–10695.
- Swanson, B. A.; Frey, P. A. Unpublished observations.
- Wong, Y.-H.; Frey, P. A. Uridine diphosphate galactose 4-epimerase. Alkylation of enzyme-bound diphosphopyridine nucleotide by p-(bromoacetamido) phenyl uridyl pyrophosphate, an active-site-directed irreversible inhibitor. *Biochemistry* **1979**, *18*, 5337–5341.
- Flentke, G. R.; Frey, P. A. The reaction of uridine diphosphate galactose 4-epimerase with a suicide inactivator. *Biochemistry* **1990**, *29*, 2430–2436.
- Berger, E.; Arabshahi, A.; Wei, Y.; Schilling, J. F.; Frey, P. A. Acid-base catalysis by UDP-galactose 4-epimerase: Correlations of kinetically measured acid dissociation constants with thermodynamic values for tyrosine 149. *Biochemistry* **2001**, *40*, 6699–6705.
- Cook, P.; Cleland, W. W. pH variation of isotope effects in enzyme-catalyzed reactions. 1. Isotope- and pH-dependent steps the same. *Biochemistry* **1981**, *20*, 1797–1805.
- Cook, P.; Cleland, W. W. pH variation of isotope effects in enzyme catalyzed reactions. 2. Isotope-dependent step not pH-dependent. Kinetic mechanism of alcohol dehydrogenase. *Biochemistry* **1981**, *20*, 1806–1816.
- Arabshahi, A.; Flentke, G. R.; Frey, P. A. Uridine diphosphate galactose 4-epimerase. pH-dependence of the reduction of NAD<sup>+</sup> by a substrate analog. *J. Biol. Chem.* **1988**, *263*, 2638–2643.
- Swanson, B. A.; Frey, P. A. Identification of lysine 153 as a functionally important residue in UDP-galactose 4-epimerase from *Escherichia coli*. *Biochemistry* **1993**, *32*, 13231–13236.
- Davis, J. E.; Nolan, L. D.; Frey, P. A. UMP-dependent reduction of UDP-galactose 4-epimerase-NAD<sup>+</sup> complex by sodium cyanoborohydride. *Biochim. Biophys. Acta* **1974**, *334*, 442–447.
- Konopka, J. M.; Halkides, C. J.; Vanhooke, J. L.; Gorenstein, D. G.; Frey, P. A. UDP-galactose 4-epimerase. Phosphorus-31 nuclear magnetic resonance analysis of NAD<sup>+</sup> and NADH bound at the active site. *Biochemistry* **1989**, *28*, 2645–2654.
- Burke, J. R.; Frey, P. A. The importance of binding energy in catalysis of hydride transfer by UDP-galactose 4-epimerase: A <sup>13</sup>C- and <sup>15</sup>N-NMR and kinetic study. *Biochemistry* **1993**, *32*, 13220–13230.

- 34 Wei, Y.; Lin, J.; Frey, P. A.  $^{13}\text{C}$ -NMR analysis of electrostatic interactions between  $\text{NAD}^+$  and active site residues of UDP-galactose 4-epimerase: Implications for the activation induced by uridine nucleotides. *Biochemistry* **2001**, *40*, 11279–11287.
- 35 Burke, J. R.; Frey, P. A. Correlation of electronic effects in N-alkylnicotinamides with NMR chemical shifts and hydride transfer reactivity. *J. Org. Chem.* **1996**, *61*, 530–533.
- 36 Liu, Y.; Arabshahi, A.; Frey, P. A. Rate enhancements brought about by uridine nucleotides in the reduction of  $\text{NAD}^+$  at the active site of UDP-galactose 4-epimerase. *Bioorg. Chem.* **2000**, *8*, 29–37.
- 37 Piller, F.; Hanlon, M. H.; Hill, R. L. Co-purification and characterization of UDP-glucose 4-epimerase and UDP-N-acetylglucosamine 4-epimerase from porcine submaxillary glands. *J. Biol. Chem.* **1983**, *258*, 10774–10778.
- 38 Thoden, J. B.; Wohlers, T. M.; Fridovich-Keil, J. L.; Holden, H. M. Human UDP-galactose 4-epimerase. Accommodation of UDP-N-acetylglucosamine within the active site. *J. Biol. Chem.* **2001**, *276*, 15131–15136.
- 39 Thoden, J. B.; Henderson, J. M.; Fridovich-Keil, J. L.; Holden, H. M. Structural analysis of the Y229C mutant of Escherichia coli UDP-galactose 4-epimerase. Teaching an old dog new tricks. *J. Biol. Chem.* **2002**, *277*, 27528–27534.
- 40 Ishiyama, N.; Creuzenet, C.; Lam, J. S.; Berghuis, A. M. Crystal structure of WbpP, a genuine UDP-N-acetylglucosamine 4-epimerase from Pseudomonas aeruginosa: Substrate specificity in UDP-hexose 4-epimerases. *J. Biol. Chem.* **2004**, *279*, 22635–22642.
- 41 Schulz, J. M.; Watson, A. L.; Sanders, R.; Ross, K. L.; Thoden, J. B.; Holden, H. M.; Fridovich-Keil, J. L. Determinants of function and substrate specificity in human UDP-galactose 4-epimerase. *J. Biol. Chem.* **2004**, *279*, 32796–32803.
- 42 Guo, H.; Li, L.; Wang, P. G. Biochemical characterization of UDP-GlcNAc/Glc 4-epimerase from Escherichia coli O86:B7. *Biochemistry* **2006**, *45*, 13760–13768.
- 43 Wong, S. S.; Frey, P. A. UDP galactose 4-epimerase catalyzed oxygen dependent reduction of a free radical substrate analogue by two electron reducing agents. *J. Am. Chem. Soc.* **1976**, *98*, 7886–7887.
- 44 Kosower, E. M.; Poziomek, E. J. Stable free radicals. I. Isolation and distillation of 1-ethyl-4-carbomethoxypyridinyl. *J. Am. Chem. Soc.* **1964**, *86*, 5515–5523.
- 45 Kosower, E. M.; Teuerstein, A.; Burrows, H. D.; Swallow, A. J. Bimolecular reactions of pyridinyl radicals in water and the mechanism of  $\text{NAD}^+$ -NADH dehydrogenase reactions. *J. Am. Chem. Soc.* **1978**, *100*, 5185–5190.
- 46 Stewart, R.; Norria, S. J. The pyridinium-dihydropyridine system. Part 2. Substituent effects on the oxidation of 1,4-dihydropyridines by flavins. *J. Chem. Soc., Perkin Trans. 2* (1972–1999) **1978**, 246–249.
- 47 Powell, M. F.; Wong, W. H.; Bruice, T. C. Concerning  $1\text{e}^-$  transfer in reduction by dihydronicotinamide reaction of oxidized flavin and flavin radical with N-benzyl-1,4-dihydronicotinamide. *Proc. Natl. Acad. Sci. U.S.A.* **1982**, *79*, 4604–4608.